Quinoa starch microspheres for drug delivery: preparation and their characteristics

Yang LUO[1], Futai NI[2], Mingzhu GUO[3], Juan LIU[4], Huan CHEN[1], Sitong ZHANG[1],
Yanli LI[1], Guang CHEN[1,5], Gang WANG[1,5*] (iD)

Abstract

Quinoa starch microparticles (QSMs) fabricated with unhydrolyzed quinoa starch (QS) by inverse microemulsion technology could be used as medicine delivery and cosmetic accessories. The size distribution of QSMs was uniform at 28.5 μM, and the adsorption capacity of methylene blue was 0.82 mg/ g. The optimum preparation process was as follows: a QS mass fraction of 9%, an epoxy chloropropane content of 1%, an amount of oil phase of 100 mL, a span 80 of 3 mg/mL, and a stirring speed of 400 r/min for 3 h at room temperature and pressure. The QSMs were spherical, ellipsoidal in shape with the specific surface area of 1.676 m^2/g. The crystallinity of the QSMs increased from 1.24% to 16.8% after crosslinking. The maximum thermal degradation temperature of the QSMs rose slightly than QS. It will be a promising material for application as a drug carrier and in cosmetics.

Keywords: quinoa starch microspheres; inverse emulsion polymerization; characteristics.

Practical Application: Applied in drug carrier and cosmetics.

1 Introduction

Starch microspheres (SMs) are micron-sized spherical particles consisting of starch chains/starch derivatives which have been widely used as drug delivery systems, embolizing agents and hemostatic agents (Chen et al., 2017; Orlacchio et al., 2020; Puncha-Arnon et al., 2020; Ee et al., 2020). SMs can be prepared by precipitation, solvent evaporation, spray-drying and emulsion techniques (Elfstrand et al., 2009; Li et al., 2009; Ma et al., 2011). The emulsion technique is one of the classic methods to obtain starch-based microparticles (Li et al., 2009; Seki et al., 2007). In the emulsifying system, soluble starch is a product mostly derived from the partial hydrolysis of potato or corn starch with acid (Lin et al., 2003; Franco et al., 2020; Khan et al., 2021; Rivera-Castro et al., 2020). It is unevenness and loss large amount of native starch after hydrolysis (Lemos et al., 2021; Li et al., 2018). Quinoa starch (QS) is the major component (50%60%) of quinoa seeds which has a small granule size (~1.5 μM), a high amylopectin content (75%96%) and a short average chain length compared with those of other starches (Dakhili et al., 2019; Jan et al., 2017; Li & Zhu, 2017; Yuan et al., 2018; Kurek & Sokolova, 2020). These structural features contribute to quinoa starch exhibiting several interesting physicochemical properties such as perfect gelation, stability, high swelling power and high enzyme susceptibility (Li et al., 2016; Srichuwong et al., 2017). Natural QS will be a propriate material for SMs without hydrolysis process. Furthermore, quinoa starch microspheres (QSMs) would be an effective method for improving its properties for value-added products development. Because of the small size of quinoa starch, microspherification is the most suitable process

for modification of quinoa starch. Especially, the microspheres have the advantages of biodegradability, good biocompatibility, a high capacity for drug carrier, slower release properties, good storage stability, no toxicity and no immune activity as well as being produced at a relatively low cost (Gross & Albrecht, 2020; Yang et al., 2010). Starch microspheres have been widely used in the pharmaceutical, food, cosmetics and other industries (Wang et al., 2015; Zheng et al., 2015). Several recent studies have investigated the preparation of starch microspheres and their physicochemical properties. For instance, a novel microsphere based on starch crosslinked with N, N'-methylenebisacrylamide (MBA) have been developed for delivering curcumin which exhibited a high loading efficiency even in loading solutions of different curcumin concentrations (Pereira et al., 2013). A study on repaglinide showed that acetylated bitter and Chinese yam starches were suitable polymers for prolonging its release in microsphere formulations (Okunlola et al., 2017). Another study on the hydration of crosslinked starch microspheres indicated that the uptake of water was accompanied by substantial swelling and changes in its polymer structure which could be used as a medical device (Wojtasz et al., 2016). Thus, these successful applications of starch microspheres in the pharmaceutical field also make them a promising candidate for application in functional foods. For example, a starch-based functional food product fortified with a lipophilic bioactive component, β-carotene in a starch hydrogel, has been prepared. The release properties were studied, showing that this product may improve human health and wellness (Mun et al., 2015). A previous study has shown

that the starch granules of quinoa are irregular polygons ranging in diameter from 1 to 3 μM, a lower crystallinity and smaller size than maize starch and potato starch, making it a suitable material for cosmetics application even after being crosslinked (Jiang et al., 2014; Orsuwan & Sothornvit, 2015; Ruales & Nair, 1994; Shin et al., 2018; Moreno et al., 2020). However, no modified products based on quinoa starch have yet been reported. Therefore, the present study aims to synthesize QSMs and investigate their structural characteristics and utilization. This investigation into QSMs will not only help to increase the value of quinoa products, but also provide a technical reference for the further processing of quinoa starch.

2 Materials and methods

2.1 Materials

The quinoa starch was provided by the Quinoa Engineering Technology Research Center of Jilin Province, China. The sodium hydroxide, methylene blue, Span 80, acetone, ethyl acetate, and anhydrous ethanol were analytically pure and purchased from the National Medicine Group Chemical Reagent Co., Ltd. (Shanghai, China). All other chemicals used in the present study were of analytical grade.

2.2 Preparation of QSMs

Different solutions of quinoa starch were prepared by adding quinoa starch (5, 6, 7, 8, 9, 10 and 11 g) to 100 mL 1 mol/L sodium hydroxide solution, followed by stirring for 30 min at 60 °C then cooling to room temperature to provide the aqueous phase (A). Soybean oil (80, 100, 120, 140, and 160 mL) was mixed with the desired amount of Span 80 (concentration of Span 80 was 1.5, 2, 2.5, 3, 3.5 and 4 mg/mL), mechanical stirring (300, 400, 500, 600 and 700 r/min) at 60 °C until the Span 80 had been dissolved. The solution was cooled to 40 °C to provide the oil phase (B). Subsequently, the aqueous phase (A) of 20 mL was added to the oil phase (B) of 80 mL with mechanical stirring to produce an inverse emulsion. After 30 min of emulsification, epoxy chloropropane (0.6, 0.8, 1.0, 1.2, and 1.4 mL) was added to the emulsion as the crosslinker for developing the microspheres. The solution was stirred for about 6 h at 40 °C and 500 r/min. The microspheres were then centrifuged at 4000 r/min to remove oil and washed with ethyl acetate, absolute alcohol, and acetone in sequence. Finally, the microspheres were dried at 40 °C for 6 h.

2.3 Orthogonal experiment

Taking the methylene blue adsorption capacity of QSMs as the reference, an orthogonal design of L$_{16}$ (4^5) was set up. The main factors used for determining the optimum preparation process of QSMs was : amount of crosslinker (a:0.6 mL, 0.8 mL, 1.0 mL, 1.2 mL); oil phase dosage (b: 60 mL, 80 mL, 100 mL, 120 mL); starch mass fraction (c: 9%; 10%; 11%; 12%); emulsifier concentration (d: 2.5 mg/mL, 3 mg/mL, 3.5 mg/mL, 4 mg/mL); and stirring speed (e: 300 r/min, 400 r/min, 500 r/min, 600 r/min) (Table S1).

2.4 Determination of adsorption properties of QSMs

Standard curve of methylene blue: methylene blue (0.01 g) was dissolved in 100 mL of distilled water. Then their absorbance

values were measured at a wavelength of 660 nm. The standard working curve equation of methylene blue was then established as: $y = 0.0597 x + 0.0087$, R^2 = 0.9967. Where y is adsorption capacity (mg/mL), and x is absorbance value. To determine the adsorption capacity of the samples, dry starch microspheres (0.2 g) were added to 20 mL of 10 mg/mL methylene blue solution then shaken on an oscillator for 2 h, followed by centrifugation at 3000 g for 5 min. The absorbance value of the supernatant was measured at 660 nm. The adsorption capacity of the QSMs were then calculated using the methylene blue regression equation above. The antibiotic adsorption experiment was carried out as follows: Batch adsorption was used to study the adsorption efficiency of QSMs. The known concentration of amoxicillin, moxifloxacin, tetracycline hydrochloride, and ciprofloxacin in aqueous solution and mass of QSMs (0.1 g) were kept in conical flasks. All the flasks containing antibiotic solutions were agitated at 100 r/min and 30 ºC. After maintaining the equilibrium, the QSMs were separated and aqueous phase concentration of antibiotic were analyzed using UV- spectrophotometer.

Determination of particle size and particle size distribution of QSMs. QSMs dissolved in absolute alcohol and dispersed using an ultrasonic bath for 2 min, adjusted to a suitable concentration then photographed under a microscope (Invitrogen EVOS FL Auto Cell Imaging System, USA). The average particle size and particle size distribution of QSMs were analyzed using a digital microscope analysis system (Mshot Image Analysis System, MC50-S, Guangzhou, China).

2.5 Structural characteristic analysis of QSMs

The microstructural changes in the QS and QSMs were observed at a high voltage (5 KV) using SEM (Carl Zeiss Jena GmbH, Jena, Germany) after the samples were coated with gold: palladium (3:1). The crystallinities of the QS and QSMs were determined by X-ray diffractometry (D8-ADVANCE, Bruker AXS GmbH, Karlsruhe, Germany) using Cu radiation (λ = 0.1541 nm) with a 2θ range of 5° to 60°. The potassium bromide press test method and Attenuated Total Reflectance Fourier Transform Infrared Spectroscopy in transmission mode (ALPHA FT-IR Spectrometer, Bruker AXS GmbH) were used to quantify the changes in the chemical bonds. Take 1-2 mg of QSMs, add pure KBr of 200 mg, then press into a transparent sheet, scanned 32 times over a wavelength range of 4000400 cm^{-1} at a resolution of 4 cm^{-1}.

Determination of surface area and average pore diameter of QS and QSMs. The pore size distribution and surface area for the QS and QSMs were measured by a physisorption apparatus (3H-2000PS1, Beishide Co. Ltd., China), the nitrogen adsorption-desorption method was employed for the surface area analyze.

2.6 N^2 adsorption experiment of QS and QSMs

The porosity of QS and QSMs was characterized by N^2 adsorption-desorption isotherms with Quantachrome Autosorb iQ2 at 77 K (N^2 adsorption/desorption isotherms, USA). The surface area was calculated based on the Brunauer–Emmett–Teller (BET).

2.7 Differential Scanning Calorimetry (DSC) and Thermogravimetric Analysis (TGA) analysis of QS and QSMs

A DSC test was carried out using 4 mg of each sample (QS and QSMs), which were hermetically sealed in an aluminum DSC pans and heat-scanning was performed at 10 °C/min in a temperature range between 50 °C and 125 °C, the ultra-pure nitrogen flow rate was 50 mL/min (SDT-Q600; TA Instruments, New Castle, USA). The TGA measurements of the QSMs were carried out using above mentioned instrument (SDT-Q600; TA Instruments, New Castle, USA). Took 4 mg of the QSMs samples, loaded into a platinum pan and heated from 30 °C to 600 °C at a heating rate of 10 °C/min under a nitrogen atmosphere with a gas flow rate of 20 mL/min.

3 Results and discussion

3.1 Preparation conditions for optimizing QSMs

Single factor and orthogonal experiments were carried out to prepare QSMs with characteristics of adsorption capacities and small particle size. The adsorption capacities of methylene blue of the QS and QSMs under different preparation conditions are shown in Figure 1. In general, the QSMs exhibited a much stronger capability of methylene blue adsorption than raw QS. The starch solutions were dispersed in the oil phase as the water phase and formed a microemulsion system through the action of the Span 80 surfactant. If the starch mass fraction is lower than 5%, a microemulsion system cannot be formed. Figure 1A shows

that the adsorption capacity for methylene blue increased at first then dropped as the starch mass fraction increased. At a starch mass fraction below 10%, the adsorption capacity increased as the starch mass fraction increased but if it increased further, the adsorption capacity decreased. Therefore, the optimum starch content was taken as 10% (Figure 1A). The amount of methylene blue adsorbed by the starch microspheres increased as the concentration of the epoxy chloropropane concentration crosslinker increased from 0.6% to 1.4% (Figure 1B). The QSMs exhibited the highest adsorption capacity at an epoxy chloropropane concentration of 1% (Figure 1B) but although the adsorption capacity improved at concentrations above 1.2% the particle size of the QSMs became too large to be used in the field of cosmetics. Therefore, the optimum crosslinker concentration was taken as 1%. Figure 1C shows that when the amount of Span 80 emulsifier was less than 2.5 mg/mL, a stable inverse suspension system could not be formed. At emulsifier concentrations between 2.5 and 3.5 mg/mL, the amount of methylene blue adsorbed by the starch microspheres increased as the Span 80 concentration increased, with the maximum adsorption capacity at 3.5 mg/mL. An excess of emulsifier will inhibit the crosslinking reaction and lead to a reduction in adsorption capacity. Therefore, the optimal emulsifier concentration was taken as 3.5 mg/mL (Figure 1C). A low oil/water ratio leads to the formation of irregular spheres during the polymerization process in the reverse microemulsion system. An excessive oil/water ratio will not only reduce the utilization ratio of the equipment and increase energy consumption, but also reduce the concentration of the crosslinker for the same amount of crosslinker, so that the quinoa starch would not be
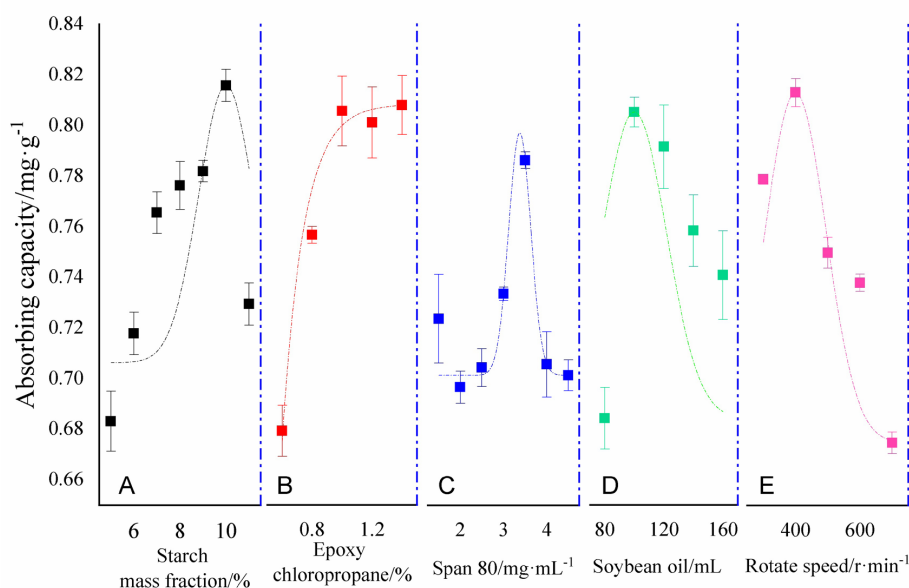
Figure 1. The effects of different treatments on the characteristics of quinoa starch microspheres: (A) 5%-11% of quinoa starch solutions 20 mL added to soybean oil 100 mL(Emulsified with 3.5 mg mL^{-1} of span 80), 1% epoxy chloropropane, stirring at 400 r min^{-1} for 6 h; (B) 10% quinoa starch solutions of 20 mL added to soybean oil 100 mL (Emulsified with 3.5 mg mL^{-1} of span 80), add 1%-1.4% epoxy chloropropane, stirring at 400 r min^{-1} for 6 h; (C) 10% quinoa starch solutions of 20 mL added to soybean oil 100 mL (Emulsified with 1.5-3.5 mg mL^{-1} of span 80), add 1% epoxy chloropropane, stirring at 400 r min^{-1} for 6 h; (D) 10% quinoa starch solutions of 20 mL added to soybean oil 80-100 mL(Emulsified with 3.5 mg mL^{-1} of span 80), add 1% epoxy chloropropane, stirring at 400 r min^{-1} for 6 h; (E) 10% quinoa starch solutions of 20 mL added to soybean oil 100 mL(Emulsified with 3.5 mg mL^{-1} of span 80), add 1% epoxy chloropropane, stirring at 300-400 r min^{-1} for 6 h.

well crosslinked. Figure 1D shows that the adsorption capacity of the starch microspheres for methylene blue increased at first then decreased as the concentration of the oil phase increased. When the amount of the oil phase was 100 mL, the adsorption capacity of the starch microspheres reached a maximum value of 0.7949 mg/g (Figure 1D). The speed of stirring is also an important factor. Figure 1E shows that an increase in the stirring speed helped to disperse the water. At a speed of less than 400 r/min, the stirring speed was correlated with the particle size and the adsorption capacity. However, at a slow stirring speed, the water droplets were not dispersed well enough to provide a sufficient adsorption capacity. At a stirring speed of 400 r/min, the maximum adsorption capacity was achieved (Figure 1D). To further optimize the preparation process, an orthogonal design was used with the results shown in Tables S2 and S3. According to the F values in Table s3, the main sequence of effects was A > D > E > B > C or crosslinker concentration > emulsifier

concentration > stirring speed > oil phase > starch mass fraction. The optimum technological parameters for each factor were A_3 $B_3 C_1 D_2 E_2$, corresponding to a crosslinker concentration of 1%, an oil phase amount of 100 mL, a starch mass fraction of 9%, an emulsifier concentration of 3 mg/mL and a stirring speed of 400 r/min. As the starch content (C) had the smallest influence on the adsorption capacity, it was used as the error item in the variance analysis table. From Table s3, $F_A > F_{0.01}$ (2,2), $F_B < F_{0.05}$ (2,2), $F_C < F_{0.05}$ (2,2), $F_D > F_{0.05}$ (2,2), and $F_E > F_{0.05}$ ($F_E > F_{0.05}$), so the crosslinker concentration had a very significant effect on the adsorption capacity of methylene blue on QSMs. Emulsifier (D) and stirring speed (E) both had significant effects on the adsorption capacity of methylene blue on QSMs. The oil phase amount (B) and starch mass fraction (C) had no significant effect on the adsorption of methylene blue on QSMs. Three experiments under the optimum conditions showed an average adsorption capacity for QSMs of 0.82 mg/g, indicating that the optimized extraction conditions were reliable.

To verify the ability of QSMs to act as a drug carrier, an antibiotic adsorption experiment was also conducted (Figure 2). It was found from Figure 2 that tetracycline hydrochloride and amoxicillin were adsorbed poorly but moxifloxacin and ciprofloxacin were better adsorbed.

3.2 Morphological and structural characterization of QSMs

The surface morphology of QS and QSMs was observed using scanning electron microscopy. The QS particles were regular polygons with a particle size of about 23 μM (Figure 3A). The QSMs were spherical, ellipsoidal or irregular in shape, with a high size polydispersity index, and were joined to other QSMs (Figure 3B), possibly caused by the emulsification method as mentioned above. When stirring at high speed, the droplets coalesced and broke up frequently during the emulsification and crosslinking processes (Figure 3B). Therefore, adhesion between microparticles could not be avoided.

The size distribution of the QSMs was uniform fairly with most particles having an average size of 28.5 μM (Figure 4 and
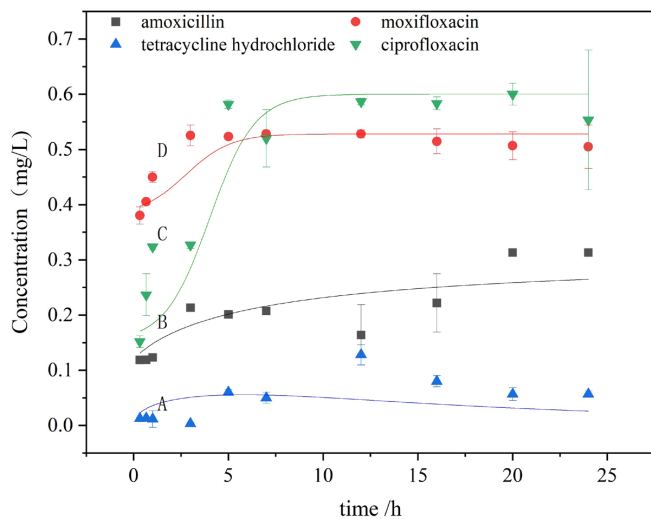
Figure 2. Drug loading capacity of QSMs: (A) tetracycline hydrochloride; (B) amoxicillin; (C) moxifloxacin; (D) ciprofloxacin. Each value is the mean of the three replicates.
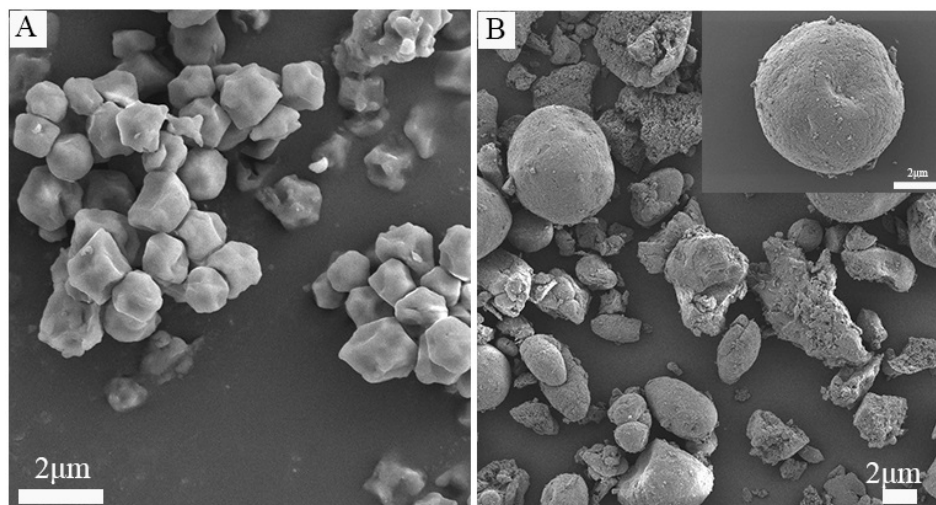
Figure 3. SEM of QS and QSMs: (A) QS; (B) QSMs.
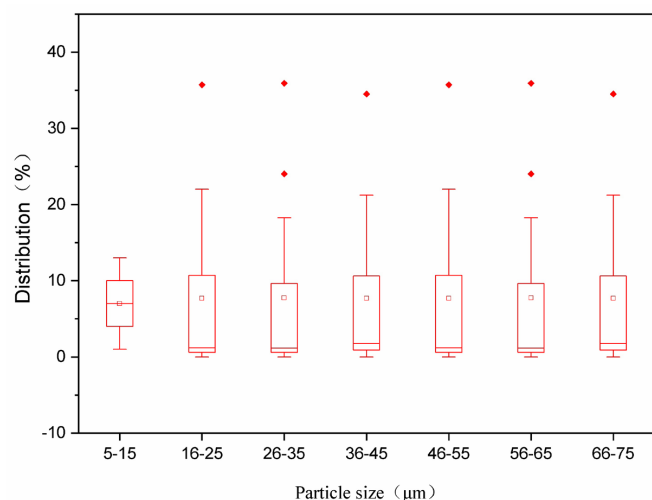
Figure 4. Particle size distribution of prepared QSMs: 9% of quinoa starch solutions 20 mL added to soybean oil 100 mL (Emulsified with 3.5 mg mL^{-1} of span 80), 1% epoxy chloropropane, stirring at 400 r min^{-1} for 6 h.

Figure S1-S5). These particles were significantly smaller than those of potato starch (44.65 µM). (Fang et al., 2020; Guo et al., 2020; Liu et al., 2020). The QSMs were prepared using food grade materials so they were non-toxic, biodegradable and smaller in size than other studies (Jiang et al., 2014; Shin et al., 2018). Therefore, they have potential for use in the field of cosmetics and as carriers of some functional flavors (Daudt et al., 2015; Rafiee et al., 2019).

The pore structures of the QSMs were analyzed regarding their specific surface area, average pore diameter and adsorption capacity (Figure 5). The specific surface area for the QSMs was 1.676 m^2/g. The highest volume adsorbed was about 8 cm^3/g which agreed with the results on pore structure and was also consistent with that from the antibiotic adsorption experiments (Figure 5).

Infrared spectroscopy is an important method for analyzing the molecular chemical bonds or functional groups of starch (Okunlola et al., 2017; Pereira et al., 2013). The structural organization of QSMs was investigated using FTIR (Figure 6). The peak between 3200-3600 cm^{-1} indicated the stretching vibration of -OH. These strong and broad -OH stretching vibration absorption bands appeared in the vicinity of 3368 cm^{-1} for QS and QSMs, which showed that -OH was present in the functional groups before and after crosslinking, but the formation of the starch microspheres reduced the association of the -OH hydrogen bonds. The bending vibration absorption peak of -OH was 1562 cm^{-1}, with the absorption peak of QSMs being significantly weaker than that of QS, indicating that some of the -OH groups in QS were crosslinked via epichlorohydrin. The QSMs were more vibrant than QS at 1150 cm^{-1} and 1356 cm^{-1}, possibly because the reaction between QS and epichlorohydrin had produced an ether bond. XRD was used to investigate the crystalline structure and the relative crystallinity of the QSMs.

The XRD patterns of the QS and QSMs samples are shown in Table 1 and Figure S6. The crystallinity of the QSMs increased
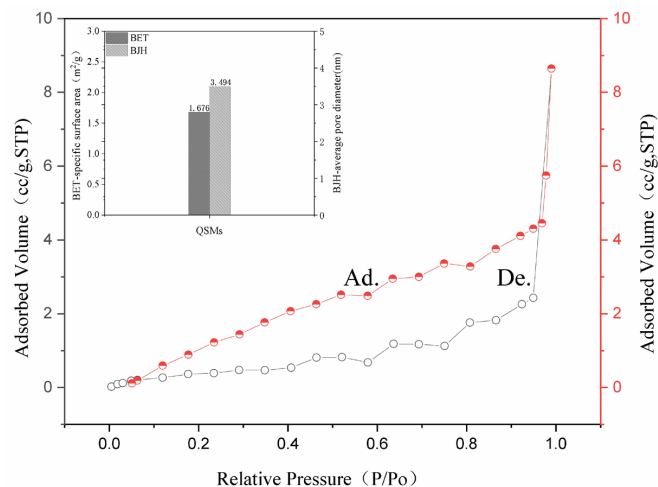
Figure 5. BET characteristic of QSMs based on N$_2$ adsorption: Ad. (adsorption); De. (desorption).
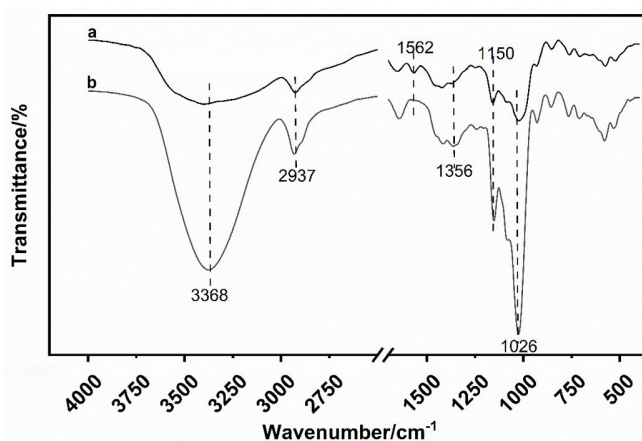
Figure 6. The FT-IR spectra of starches: (a) QS; (b) QSMs.

Table 1. XRD analysis of QS and QSMs.

Sample	Crystallinity index (CrI) (Mean ± SD, %)
QS	1.24 ± 0.08
QSMs	16.8 ± 0.07

from 1.24% to 16.8% after crosslinking (Table 1, Figure S6). Strong diffraction peaks were observed at 15.1°, 17.1°, and 23.1° for the QSMs, which is same as others (Contreras-Jiménez et al., 2019; Valdez-Arana et al., 2020). This occurred because the starch chains were in disorder after crosslinking, which weakened the interaction between the molecules and hydrogen bonds, resulting in an increase in the crystallinity of the starch and a reduction in the crystalline regions (Li et al., 2019).

3.3 Thermal analysis of QSMs

The results of the thermal analysis of QS and QSMs are shown in Figure 7. Figure 7A shows the DSC thermograms of QS and QSMs. The DSC curve (Figure 7a) shows an endothermic peak with values for QS and QSMs at 98 °C and 100 °C respectively, mainly due to water evaporation from the QS and QSMs
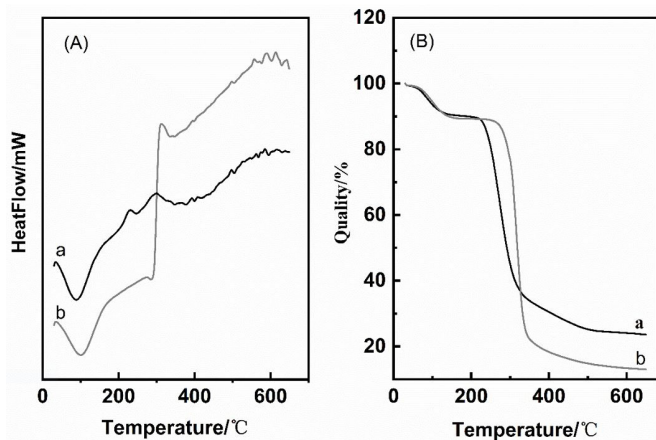
Figure 7. Thermal analysis of starches: (a) quinoa starch; (b) quinoa starch microsphere. (A) DSC spectra of starches; (B) TG spectra of starches.

(Figure 7A). The endothermic peak for QS at 284.1 and 294.1 °C could mainly be attributed to the C-C bond breakage. The peak for QSMs at 224.8 °C, may have been caused by the effect of crosslinking between the starch and the crosslinker, leading to a decrease in the crystallinity of the microspheres. This result shows the different application where the material can be used. From the TGA curve (Figure 7b), the thermogravimetric loss of QS mainly ranged from 230 °C to 300 °C, and the maximum thermal degradation temperature was 300.1 °C (Figure 7B). The degradation temperature of QSMs ranged from 260 °C to 352 °C, and the maximum degradation temperatures were from 342.7 °C. Compared with QS, the maximum thermal degradation temperature of the QSMs prepared by cross-linked rose slightly. It may be that, after crosslinking, the starch granules leave compact crystalline regions.

4 Conclusions

The QSMs have been prepared for the first time using epichlorohydrin as the crosslinker and were synthesized through inverse emulsion polymerization. The QSMs were comparatively small, and more spherical than QS. The good adsorption performance of QSMs was confirmed by experiments using methylene blue and different antibiotics. The optimum preparation process was as follows: a QS mass fraction of 9%, an epichlorohydrin concentration of 1%, an oil amount of 100 mL, a span 80 concentration of 3 mg/mL and stirring at 400 r/min for 3 h at room temperature and pressure. The FTIR and XRD spectroscopy results confirmed that the QSMs had been synthesized successfully. The crystallinity of QSMs decreased significantly, and their adsorption properties and thermal stability were significantly improved compared with those for QS. The present study has provided a good theoretical basis for the application of QSMs as drug carriers, adsorbent carriers and for use in cosmetics.

Conflict of interest

The authors declare no conflict of interest.

References

Chen, F., Cao, X., Yu, J., Su, H., Wei, S., Hong, H., & Liu, C. (2017). Quaternary ammonium groups modified starch microspheres for instant hemorrhage control. *Colloids and Surfaces. B, Biointerfaces*, 159, 937-944. http://dx.doi.org/10.1016/j.colsurfb.2017.08.024. PMid:28922716.

Contreras-Jiménez, B., Torres-Vargas, O. L., & Rodríguez-García, M. E. (2019). Physicochemical characterization of quinoa (Chenopodium quinoa) flour and isolated starch. *Food Chemistry*, 298, 124982. http://dx.doi.org/10.1016/j.foodchem.2019.124982. PMid:31261014.

Dakhili, S., Abdolalizadeh, L., Hosseini, S. M., Shojaee-Aliabadi, S., & Mirmoghtadaie, L. (2019). Quinoa protein: composition, structure and functional properties. *Food Chemistry*, 299, 125161. http://dx.doi.org/10.1016/j.foodchem.2019.125161. PMid:31323439.

Daudt, R. M., Back, P. I., Cardozo, N. S. M., Marczak, L. D. F., & Külkamp-Guerreiro, I. C. (2015). Pinhão starch and coat extract as new natural cosmetic ingredients: topical formulation stability and sensory analysis. *Carbohydrate Polymers*, 134, 573-580. http://dx.doi.org/10.1016/j.carbpol.2015.08.038. PMid:26428160.

Ee, K. Y., Eng, M. K., & Lee, M. L. (2020). Physicochemical, thermal and rheological properties of commercial wheat flours and corresponding starches. *Food Science and Technology*, 40(Suppl. 1), 51-59. http://dx.doi.org/10.1590/fst.39718.

Elfstrand, L., Eliasson, A.-C., & Wahlgren, M. (2009). Changes in starch structure during manufacturing of starch microspheres for use in parenteral drug formulations: Effects of temperature treatment. *Carbohydrate Polymers*, 75(1), 157-165. http://dx.doi.org/10.1016/j.carbpol.2008.07.018.

Fang, F., Luo, X., BeMiller, J. N., Schaffter, S., Hayes, A. M. R., Woodbury, T. J., Hamaker, B. R., & Campanella, O. H. (2020). Neutral hydrocolloids promote shear-induced elasticity and gel strength of gelatinized waxy potato starch. *Food Hydrocolloids*, 107, 105923. http://dx.doi.org/10.1016/j.foodhyd.2020.105923.

Franco, V. A., Garcia, L. G. C., & Silva, F. A. (2020). Addition of hydrocolidics in gluten-free bread and replacement of rice flour for sweet potato flour. *Food Science and Technology*, 40(Suppl. 1), 88-96. http://dx.doi.org/10.1590/fst.05919.

Gross, A., & Albrecht, T. (2020). Transarterial Chemoembolisation (TACE) with Degradable Starch Microspheres (DSM) and anthracycline in patients with locally extensive Hepatocellular Carcinoma (HCC): safety and efficacy. *Cardiovascular and Interventional Radiology*, 43(3), 402-410. http://dx.doi.org/10.1007/s00270-019-02364-w. PMid:31705244.

Guo, Z., Han, L., Yu, Q., & Lin, L. (2020). Effect of a sea buckthorn pomace extract-esterified potato starch film on the quality and spoilage bacteria of beef jerky sold in supermarket. *Food Chemistry*, 326, 127001. http://dx.doi.org/10.1016/j.foodchem.2020.127001. PMid:32416417.

Jan, K. N., Panesar, P. S., Rana, J. C., & Singh, S. (2017). Structural, thermal and rheological properties of starches isolated from Indian quinoa varieties. *International Journal of Biological Macromolecules*, 102, 315-322. http://dx.doi.org/10.1016/j.ijbiomac.2017.04.027. PMid:28396270.

Jiang, T., Wu, C., Gao, Y., Zhu, W., Wan, L., Wang, Z., & Wang, S. (2014). Preparation of novel porous starch microsphere foam for loading and release of poorly water soluble drug. *Drug Development and Industrial Pharmacy*, 40(2), 252-259. http://dx.doi.org/10.3109/03639045.2012.756511. PMid:23391363.

Khan, F. A., Arshad, M. U., Rizvi, S. S. H., Ameer, K., Anjum, F. M., Imran, M., & Imran, A. (2021). Optimization of potato starch gel formulation as green alternative of animal-sourced gelatin. *Food Science and Technology*, 41(3), 626-634. http://dx.doi.org/10.1590/fst.24120.

Kurek, M. A., & Sokolova, N. (2020). Optimization of bread quality with quinoa flour of different particle size and degree of wheat flour replacement. *Food Science and Technology*, 40(2), 307-314. http://dx.doi.org/10.1590/fst.38318.

Lemos, P. V. F., Marcelino, H. R., Cardoso, L. G., Souza, C. O., & Druzian, J. I. (2021). Starch chemical modifications applied to drug delivery systems: from fundamentals to FDA-approved raw materials. *International Journal of Biological Macromolecules*, 184, 218-234. http://dx.doi.org/10.1016/j.ijbiomac.2021.06.077. PMid:34144062.

Li, B.-Z., Wang, L.-J, Li, D., Bhandari, B., Li, S.-J., Lan, Y., Chen, X. D., & Mao, Z.-H. (2009). Fabrication of starch-based microparticles by an emulsification-crosslinking method. *Journal of Food Engineering*, 92(3), 250-254. http://dx.doi.org/10.1016/j.jfoodeng.2008.08.011.

Li, B.-Z., Xian, X.-Q., Wang, Y., Adhikari, B., & Chen, D. (2018). Production of recrystallized starch microspheres using water-in-water emulsion and multiple recycling of polyethylene glycol solution. *Lebensmittel-Wissenschaft & Technologie*, 97, 76-82. http://dx.doi.org/10.1016/j.lwt.2018.06.034.

Li, G., & Zhu, F. (2017). Molecular structure of quinoa starch. *Carbohydrate Polymers*, 158, 124-132. http://dx.doi.org/10.1016/j.carbpol.2016.12.001. PMid:28024535.

Li, G., Wang, S., & Zhu, F. (2016). Physicochemical properties of quinoa starch. *Carbohydrate Polymers*, 137, 328-338. http://dx.doi.org/10.1016/j.carbpol.2015.10.064. PMid:26686137.

Li, S., Zhang, B., Tan, C. P., Li, C., Fu, X., & Huang, Q. (2019). Octenylsuccinate quinoa starch granule-stabilized Pickering emulsion gels: preparation, microstructure and gelling mechanism. *Food Hydrocolloids*, 91, 40-47. http://dx.doi.org/10.1016/j.foodhyd.2019.01.001.

Lin, J.-H., Lee, S.-Y., & Chang, Y.-H. (2003). Effect of acid–alcohol treatment on the molecular structure and physicochemical properties of maize and potato starches. *Carbohydrate Polymers*, 53(4), 475-482. http://dx.doi.org/10.1016/S0144-8617(03)00145-0.

Liu, P., Fang, Y., Zhang, X., Zou, F., Gao, W., Zhao, H., Yuan, C., & Cui, B. (2020). Effects of multienzyme treatment on the physicochemical properties of maize starch-lauric acid complex. *Food Hydrocolloids*, 107, 105941. http://dx.doi.org/10.1016/j.foodhyd.2020.105941.

Ma, U. V. L., Floros, J. D., & Ziegler, G. R. (2011). Effect of starch fractions on spherulite formation and microstructure. *Carbohydrate Polymers*, 83(4), 1757-1765. http://dx.doi.org/10.1016/j.carbpol.2010.10.041.

Moreno, H. M., Tovar, C. A., Domínguez-Timón, F., Cano-Báez, J., Díaz, M. T., Pedrosa, M. M., & Borderías, A. J. (2020). Gelation of commercial pea protein isolate: effect of microbial transglutaminase and thermal processing. *Food Science and Technology*, 40(4), 800-809. http://dx.doi.org/10.1590/fst.19519.

Mun, S., Kim, Y.-R., Shin, M., & McClements, D. J. (2015). Control of lipid digestion and nutraceutical bioaccessibility using starch-based filled hydrogels: influence of starch and surfactant type. *Food Hydrocolloids*, 44, 380-389. http://dx.doi.org/10.1016/j.foodhyd.2014.10.013.

Okunlola, A., Adebayo, A. S., & Adeyeye, M. C. (2017). Development of repaglinide microspheres using novel acetylated starches of bitter and Chinese yams as polymers. *International Journal of Biological Macromolecules*, 94(Pt A), 544-553. http://dx.doi.org/10.1016/j.ijbiomac.2016.10.032. PMid:27769931.

Orlacchio, A., Chegai, F., Roma, S., Merolla, S., Bosa, A., & Francioso, S. (2020). Degradable starch microspheres transarterial chemoembolization (DSMs-TACE) in patients with unresectable hepatocellular carcinoma (HCC): long-term results from a single-center 137-patient cohort prospective study. *La Radiologia Medica*, 125(1), 98-106. http://dx.doi.org/10.1007/s11547-019-01093-x. PMid:31583558.

Orsuwan, A., & Sothornvit, R. (2015). Effect of miniemulsion cross-linking and ultrasonication on properties of banana starch. *International Journal of Food Science & Technology*, 50(2), 298-304. http://dx.doi.org/10.1111/ijfs.12626.

Pereira, A. G. B., Fajardo, A. R., Nocchi, S., Nakamura, C. V., Rubira, A. F., & Muniz, E. C. (2013). Starch-based microspheres for sustained-release of curcumin: preparation and cytotoxic effect on tumor cells. *Carbohydrate Polymers*, 98(1), 711-720. http://dx.doi.org/10.1016/j.carbpol.2013.06.013. PMid:23987403.

Puncha-Arnon, S., Wandee, Y., Uttapap, D., Puttanlek, C., & Rungsardthong, V. (2020). The effect of hydrolysis of cassava starch on the characteristics of microspheres prepared by an emulsification-crosslinking method. *International Journal of Biological Macromolecules*, 161, 939-946. http://dx.doi.org/10.1016/j.ijbiomac.2020.06.122. PMid:32553976.

Rafiee, Z., Nejatian, M., Daeihamed, M., & Jafari, S. M. (2019). Application of curcumin-loaded nanocarriers for food, drug and cosmetic purposes. *Trends in Food Science & Technology*, 88, 445-458. http://dx.doi.org/10.1016/j.tifs.2019.04.017.

Rivera-Castro, V. M., Muy-Rangel, M. D., Gutiérrez-Dorado, R., Escobar-Álvarez, J. L., Hernández-Castro, E., & Valenzuela-Lagarda, J. L. (2020). Nutritional, physicochemical and anatomical evaluation of creole corn varieties from the region of the Costa Chica of Guerrero. *Food Science and Technology*, 40(4), 938-944. http://dx.doi.org/10.1590/fst.20919.

Ruales, J., & Nair, B. M. (1994). Properties of starch and dietary fibre in raw and processed quinoa (Chenopodium quinoa, Willd) seeds. *Plant Foods for Human Nutrition*, 45(3), 223-246. http://dx.doi.org/10.1007/BF01094092. PMid:8052579.

Seki, T., Shinohara, K., Kato, N., Uchida, M., Natsume, H., Morimoto, K., & Juni, K. (2007). A novel preparation method for microspheres of water soluble polymers using polypropyleneglycol as the dispersion medium. *Chemical & Pharmaceutical Bulletin*, 55(3), 403-406. http://dx.doi.org/10.1248/cpb.55.403. PMid:17329880.

Shin, S., Lee, K., Yaqoob, Z., So, P. T. C., & Park, Y. (2018). Reference-free polarization-sensitive quantitative phase imaging using single-point

optical phase conjugation. *Optics Express*, 26(21), 26858-26865. http://dx.doi.org/10.1364/OE.26.026858. PMid:30469763.

Srichuwong, S., Curti, D., Austin, S., King, R., Lamothe, L., & Gloria-Hernandez, H. (2017). Physicochemical properties and starch digestibility of whole grain sorghums, millet, quinoa and amaranth flours, as affected by starch and non-starch constituents. *Food Chemistry*, 233, 1-10. http://dx.doi.org/10.1016/j.foodchem.2017.04.019. PMid:28530552.

Valdez-Arana, J. D., Steffolani, M. E., Repo-Carrasco-Valencia, R., Pérez, G. T., & Condezo-Hoyos, L. (2020). Physicochemical and functional properties of isolated starch and their correlation with flour from the Andean Peruvian quinoa varieties. *International Journal of Biological Macromolecules*, 147, 997-1007. http://dx.doi.org/10.1016/j.ijbiomac.2019.10.067. PMid:31743707.

Wang, S., Chen, Y., Liang, H., Chen, Y., Shi, M., Wu, J., Liu, X., Li, Z., Liu, B., Yuan, Q., & Li, Y. (2015). Intestine-specific delivery of hydrophobic bioactives from oxidized starch microspheres with an enhanced stability. *Journal of Agricultural and Food Chemistry*, 63(39), 8669-8675. http://dx.doi.org/10.1021/acs.jafc.5b03575. PMid:26414436.

Wojtasz, J., Carlstedt, J., Fyhr, P., & Kocherbitov, V. (2016). Hydration and swelling of amorphous cross-linked starch microspheres. *Carbohydrate Polymers*, 135, 225-233. http://dx.doi.org/10.1016/j.carbpol.2015.08.085. PMid:26453872.

Yang, Y., Wei, X., Sun, P., & Wan, J. (2010). Preparation, characterization and adsorption performance of a novel anionic starch microsphere. *Molecules*, 15(4), 2872-2885. http://dx.doi.org/10.3390/molecules15042872. PMid:20428085.

Yuan, Y., Zhai, R., Li, Y., Chen, X., & Jin, M. (2018). Developing fast enzyme recycling strategy through elucidating enzyme adsorption kinetics on alkali and acid pretreated corn stover. *Biotechnology for Biofuels*, 11(1), 316. http://dx.doi.org/10.1186/s13068-018-1315-5. PMid:30479661.

Zheng, J., Wang, Y., Feng, Z., Kuang, Z., Zhao, D., & Jiao, X. (2015). Preparation of cationic starch microspheres and study on their absorption to anionic-type substance. *Water Science and Technology*, 71(10), 1545-1553. http://dx.doi.org/10.2166/wst.2015.137. PMid:26442497.

Supplementary material

Supplementary information associated with this article can be found in the online version.

Table S1. The L16 (45) orthogonal design.

Table S2. Orthogonal test results and analysis of preparation of QSMs.

Table S3. Variance Analysis of orthogonal experiment.

Figure S1. Effect of starch mass fraction on the particle size distribution (5%-11% of quinoa starch solutions 20 mL added to soybean oil 100 mL(Emulsified with 3.5 mg mL-1 of span 80), 1% epoxy chloropropane, stirring at 400 r min-1 for 6 h).

Figure S2. Effect of epoxy chloropropane concentration on the particle size distribution(10% quinoa starch solutions of 20 mL added to soybean oil 100 mL (Emulsified with 3.5 mg mL-1 of span 80), add 1%-1.4% epoxy chloropropane, stirring at 400 r min-1 for 6 h).

Figure S3. Effect of stirring speed on the particle size distribution (10% quinoa starch solutions of 20 mL added to soybean oil 100 mL (Emulsified with 3.5 mg mL-1 of span 80), add 1% epoxy chloropropane, stirring at 300-400 r min-1 for 6 h).

Figure S4. Effect of span concentration on the particle size distribution (10% quinoa starch solutions of 20 mL added to soybean oil 100 mL (Emulsified with 1.5-3.5 mg mL-1 of span 80), add 1% epoxy chloropropane, stirring at 400 r min-1 for 6 h).

Figure S5. Effect of oil amount on the particle size distribution (10% quinoa starch solutions of 20 mL added to soybean oil 80-100 mL (Emulsified with 3.5 mg mL-1 of span 80), add 1% epoxy chloropropane, stirring at 400 r min-1 for 6 h).

Figure S6. X-ray diffraction patterns of starches: (a) QS; (b) QSMs.

Figure S7. DSC of QS.

Figure S8. DSC of QSMs.

Figure S9. TG of QS.

Figure S10. TG of QSMs.

This material is available as part of the online article from https://www.scielo.br/j/cta